

Article

Fully Distributed, Event-Triggered Containment Control of Multi-Agent Systems Based on Wireless Sensor Networks and Time Base Generators

Lei Wang ¹, Guanwen Chen ², Tai Li ^{1,*} and Ruitian Yang ^{1,*}¹ School of Automation, Wuxi University, Wuxi 214105, China; leiwang@cw Xu.edu.cn² School of Automation, Nanjing University of Information Science and Technology, Wuxi 214105, China; guanwenchen@88.com

* Correspondence: taili@cw Xu.edu.cn (T.L.); yangruitian@cw Xu.edu.cn (R.Y.)

Abstract: In this study, wireless sensor networks and time base generators are used to solve the fixed-time containment control problem in multi-agent systems with fixed topologies. A new event-triggered control protocol is proposed, which combines a fully distributed method and a time base generator (TBG). The goal is to converge the states of all followers to the convex hull formed by the leader. The controller reduces communication and improves control efficiency by integrating a fully distributed control mechanism using wireless sensor networks. In addition, a time base generator (TBG) is added to ensure that the dwell time continues to be pre-specified and independent of initial conditions. Using matrix theory, the original system is transformed into an error system, and its stability is analyzed by the Lyapunov method. The necessary and sufficient conditions for solving the time consensus containment control problem in multi-agent systems are determined and Zeno behavior is avoided. The effectiveness of the proposed control algorithm is illustrated by numerical examples.

Keywords: actual fixed-time consensus; event-triggered control; wireless sensor networks; time base generator; containment control



Citation: Wang, L.; Chen, G.; Li, T.; Yang, R. Fully Distributed,

Event-Triggered Containment Control of Multi-Agent Systems Based on Wireless Sensor Networks and Time Base Generators. *Appl. Sci.* **2023**, *13*, 11039. <https://doi.org/10.3390/app131911039>

Academic Editor: Alessandro Lo Schiavo

Received: 19 July 2023

Revised: 25 September 2023

Accepted: 28 September 2023

Published: 7 October 2023



Copyright: © 2023 by the authors. Licensee MDPI, Basel, Switzerland. This article is an open access article distributed under the terms and conditions of the Creative Commons Attribution (CC BY) license (<https://creativecommons.org/licenses/by/4.0/>).

1. Introduction

Wireless sensor networks and system collaborations with multiple agents [1] can be combined to handle complexity, improve system performance, and use wireless sensor networks in a variety of contexts. This integration not only advances the field of control but also provides more possibilities for practical applications. The collaborative control of multi-agent systems involves interactions and cooperation among multiple agents, requiring the overcoming of challenges such as heterogeneity and uncertainty. The realm of control, such as cluster control [2–4] and formation control [5–7], has been a significant issue because it involves the interaction and cooperation between multiple agents, needs to solve complexity, optimize system performance, apply to a wide range of fields, and overcome challenges such as heterogeneity and uncertainty, so as to promote the development and practical application of the control field containment control [8–12], etc. The goal of containment control is to promote collaboration and cooperation in the multi-agent system, emphasize respect for the objectives of each agent when resolving conflicts and coordinating decisions, and seek to maximize common interests. All states of followers must converge to the leaders' convex hull. The consistency problem under study is also known as containment control when the multi-agent system contains a large number of leaders. A high-frequency feedback was proposed in reference [4]. This involved clustering for a multi-agent system with an unknown parameter in robust control. Reference [5] studied the issues of distributed simultaneous estimation and formation control within the same population of mobile agents with limited communication, perception, and computing

capabilities. A novel scalable algorithm was proposed, achieving convergence of global formation statistics and the decoupling of estimation and control performance. Reference [8] investigated how to control confinement in a second-order linear multi-agent system. We investigated a time-varying triggering threshold event-triggered control technique that takes both uniform and irregular input delays into account. The general linear multi-agent system's creation, containment, and constraint tracking under time-varying control inputs were explored in reference [13]. It proposes a formation containment-tracking protocol that achieves formation, containment, and constraint tracking of intelligent agents by considering the influence of neighboring relative information and unknown inputs from tracking leaders. Reference [14] investigated the nonlinear multi-agent system's finite time constraint control problem, and used fuzzy logic systems to approximate system dynamics. By using nonlinear transformation functions to transform state constraints into unconstrained ones, the follower's convex hull is converged in a finite amount of time using adaptive fuzzy control. In [15], the convergence time of the average consensus problem for networks with heterogeneous random link failures is studied and the influence of event-triggered communication on consensus performance is considered. A large number of simulations are carried out to verify the reliability of the method. In [16], inspired by the cooperative control, a fully distributed and delay-tolerant secondary control scheme is developed for the droop-controlled AC microgrid. The hierarchical control structure of the distributed energy unit is considered to ensure the active power sharing between the three DER units.

This article examines numerous control protocols in order to adapt to distinct needs and application histories. Based on the switching topology, reference [17] studied the event-triggered dichotomous consistency of multi-agent systems. In [18], for a class of strict feedback nonlinear systems with external disturbances, a robust fuzzy adaptive prescribed performance finite-time control strategy based on event-triggering is proposed. The event-triggered signal based on a relative threshold is introduced to reduce the communication burden, and the dynamic surface control technology is used to solve the problem of computational complexity. In response to the need to reduce the frequency of event triggering, reference [19] introduced a dynamic event-triggering mechanism that optimizes the utilization of communication resources via internal dynamic variables. This mechanism can adaptively adjust event-triggering conditions based on changes in the system state, thus more effectively achieving consistency control objectives [20]. This further proves that the dynamic event-triggering method can significantly reduce communication overhead and improve system stability and performance. Referring to [21], it was determined how backstepping controllers affect parameter uncertainty and how they are used to manage the fixed-time creation of a heterogeneous multi-agent system. Reference [22] applies the integral to create a sliding mode using a sliding mode control mechanism controller, considering the effects of external interference. Multi-agent systems typically have constrained communication resources in real-world applications. Discontinuous control techniques can conserve energy and cut back on communication. Reference [23] investigated the fuzzy distributed impulsive control in the nonlinear multi-agent system protocol and achieved system consistency with regard to denial-of-service (DoS) assaults. Multi-agent systems, including [24,25], have extensively exploited event-triggered control techniques. Reference [24] studied the distributed two-part tracking control protocol based on event triggering for a stochastic multi-agent nonlinear system with input saturation. By constructing a novel observer and adopting an event-triggering mechanism, boundedness and distributed consistency tracking of signals were achieved. For linear multi-agent systems, reference [25] put forth a fully distributed event-triggered control approach. In addition, control protocols can also be used to achieve self-triggering. Reference [26] studied the robust synchronization problem of a class of master-slave neural networks with network-induced delays, unknown time-varying uncertainties, and exogenous disturbances, and developed an event-triggered control protocol to obtain the synchronization of

MSNNs. While the aforementioned literature references do consider event triggering to reduce communication, they do not specify the timing.

In order to correct the issue where the convergence time of multi-agent systems depends on initial conditions, it is crucial to conduct research on the timing control issues associated with multi-agent systems. The event-triggered controller utilizing sliding mode control technology was suggested in reference [27] in order to achieve the timing consensus of the leader polling multi-agent system. A high-order leader–follower multi-agent system’s fixed-time technique was examined in reference [28] to assess the leadership state and arrive at a tracking consensus simultaneously, and reference [29] further discussed how to implement the fixed-time strategy in the face of unknown interference. In reference [30], the weighted directed topology-based fixed-time consistent tracking control issue of second-order multi-agent systems with bounded input uncertainty was examined. Fast and stable consistency tracking control has been achieved by forming unique non-singular fast terminal sliding with fixed-time surfaces and distributed control protocols. Reference [31] investigated how a multi-agent system’s fixed-time group consistency was affected by external interference and constructed two fixed-time guidance control algorithms for the system. References [32,33] discussed the fixed-time consistency of two different forms of multi-agent systems. Regarding a first-order heterogeneous multi-agent system that is nonlinear to achieve timing consistency, reference [32] provided a new protocol design framework. Reference [33] explored the distributed fixed-time observer and fixed-time tracking controller of heterogeneous multi-agent systems. For the integrator-based multi-agent system, reference [34] proposed a fixed-time consensus technology based on TBG, which has more advantages than traditional fixed-time consensus technology. The above literature has taken into account the introduction of fixed time in order to better achieve the control objectives, but the method adopted has yet to be improved. Therefore, this paper studies the combination of the time base generator and event triggering.

This article’s primary contributions can be summed up in two ways. (1) We discussed the containment control protocol based on TBG and achieved practical timing consensus. The confinement control protocol is an efficient solution to the multi-agent system’s temporal consensus issue because it can indicate the system’s settling time in advance and reduce the initial control input. (2) A fully distributed event-triggered control mechanism was used in the architecture of the control protocol to reduce system utilization. In this mechanism, each controller samples only based on local information and does not require global information. Once the leader has created a convex hull using a fully distributed technique, the controller ultimately modifies the state of the followers to match it. This control method not only enhances the system’s robustness and collaboration but also elevates the efficacy of the system.

The following is the structure for the remaining portions of this paper: The second segment addresses a few key ideas and provides a thorough description of the issue. The third section describes the proposed containment control protocol, including TBG and a fully distributed event-triggered control mechanism, and validates the theoretical findings presented in the fourth section with simulation examples. The fifth and final section concludes by summarizing the findings.

Symbols: The notations $R^{n \times m}$ and R^n represent $n \times m$ and real moments. $\|\cdot\|$ denotes a vector’s Euclidean norm. $\lambda_{\max(\cdot)}$ and $\lambda_{\min(\cdot)}$ designate the matrix’s maximum and minimum eigenvalues, respectively. \otimes is a representation of the Kronecker product. I_n denotes an $n \times n$ identity matrix. The identity matrix is a square matrix with 1’s on the diagonal and 0’s everywhere else. A diagonal matrix is represented by $diag(\cdot)$.

2. Preliminary Knowledge and a Description of the Issue

2.1. Graph Theory

This article utilizes directed sign graphs $\mathcal{G} = \{\mathcal{V}, \mathcal{E}, \mathcal{A}\}$. The symbolic graph $\mathcal{G} = \{\mathcal{V}, \mathcal{E}, \mathcal{A}\}$ represents the N -agent communication topology. Here, the node set $\mathcal{V} = \{\mathcal{V}_1, \mathcal{V}_2, \dots, \mathcal{V}_N\}$, the edge set $\mathcal{E} \subseteq \mathcal{V} \times \mathcal{V}$ and the adjacency matrix $\mathcal{A} = (a_{ij}) \in \mathbb{R}^{N \times N}$.

The self-loop assumption states that there are no self-loops in the topology of the network, specifically, $a_{ii} = 0$ for $i = 1, \dots, N$. The following definition applies to the Laplacian matrix $\mathcal{L} = (l_{ij}) \in \mathbb{R}^{N \times N}$: $l_{ii} = \sum_{j=1, j \neq i}^N |a_{ij}|$ and $l_{ij} = -a_{ij}$ for $(i \neq j)$. If there is a path connecting any two different nodes in the graph, it is said that the graph \mathcal{G} is totally linked. The expression $(i, j) \in E$ indicates that agent i can receive information from agent j . If the directed symbolic graph \mathcal{G} contains a root node that can reach all other nodes, the directed spanning tree is said to be present.

Assumption 1. *Structure-wise, \mathcal{G} is a balanced directed sign graph.*

2.2. Time Base Generator

The function known as the time base generator (TBG) can be continuously differentiated, where certain requirements must be met by both the original and first-order time derivative.

Definition 1 ([35]). *The continuous differentiable function $\zeta(t)$ satisfies the following characteristics:*

- if $t \in [0, +\infty)$, $\zeta(t)$ is a minimum of C^2 .
- When time first begins, $t_0 = 0$, and at the time moment t_f , the value of $\zeta(t)$ satisfies $\zeta(0) = 0$, $\zeta(t_f) = 1$, and $\zeta(t)$ is a function that does not decrease.
- The initial derivative of $\zeta(t)$'s temporal function at the instant $t = 0$ and at t_f satisfies $\lim_{t \rightarrow 0^+} \frac{d\zeta(t)}{dt} = 0$ and $\lim_{t \rightarrow t_f} \frac{d\zeta(t)}{dt} = 0$.
- When $t \in [t_f, +\infty)$, $\zeta(t)$ and $\dot{\zeta}(t)$ maintain the same, where $\zeta(t) = 1$ and $\dot{\zeta}(t) = 0$.
TBG is corresponding to function $\zeta(t)$ in this case.

Lemma 1 ([36]). *Think of a dynamic model where the system status is indicated as $p(t) \in \mathbb{R}$, which can be said in the following manner:*

$$\dot{p}(t) = -k(t) \cdot p(t), \quad p(0) = p_0 \tag{1}$$

The TBG gain, denoted by $k(t)$, aims to

$$k(t) = \frac{\dot{\zeta}(t)}{1 - \zeta(t) + \delta} \tag{2}$$

where $\zeta(t)$ is the TBG and the known constant δ satisfies the condition $0 < \delta \ll 1$. The result is that $p(t_f) = \frac{\delta}{1+\delta} p_0$.

Remark 1. *A time base generator provides an accurate time signal that serves as a reference for the timing of multiple agents within a multi-agent system. By synchronizing the time base generator with the individual agents, it ensures that they maintain a consistent time reference during task execution and interaction. In comparison to traditional fixed-time control approaches, time base generators offer enhanced accuracy, stability, and flexibility. They can adapt to dynamic environments and the specific demands of multi-agent systems, thereby facilitating time synchronization and bolstering system consistency and reliability.*

2.3. Problem Description

In this study, we address the case of several leaders within an N -agent linear multi-agent system, where M ($M < N$) agents are followers and the leaders constitute the remaining $N - M$ agents. We specify the set of leaders as $E = \{M + 1, \dots, N\}$ and the set of followers as $F = \{1, \dots, M\}$.

The following is a representation of the dynamics of the follower i :

$$\dot{x}_i(t) = Ax_i(t) + Bu_i(t), \quad i \in F \tag{3}$$

where the status and input controls for agent i are represented by $x_i(t)$ and $u_i(t)$, respectively, in \mathbb{R}^{n_x} and \mathbb{R}^{n_u} . Matrices $A \in \mathbb{R}^{n_x \times n_x}$ and $B \in \mathbb{R}^{n_x \times n_u}$ are system matrices.

Assumption 2. (A, B) is a stable matrix.

For each leader, assuming their control input is $u_i(t) = 0$, the dynamics equation for the leaders can be stated as follows:

$$\dot{x}_i(t) = Ax_i(t), \quad i \in E \tag{4}$$

In the given equation, $x_i(t) \in \mathbb{R}^{n_x}$ is an indication of the leaders' condition. Since the leaders do not have neighbors, the \mathcal{G} Laplacian matrix of the graph can be broken down into:

$$L = \begin{bmatrix} L_1 & L_2 \\ 0_{(N-M) \times M} & 0_{(N-M) \times (N-M)} \end{bmatrix} \tag{5}$$

where L_1 is expressed in $\mathbb{R}^{M \times M}$ and L_2 is expressed in $\mathbb{R}^{M \times (N-M)}$. Furthermore, matrix L_1 represents the information flow between the M followers, and the information flow from the $N - M$ leaders to the M followers is represented by matrix L_2 .

Assumption 3. To ensure how connected graph \mathcal{G} is, each follower must have a guided path to at least one leader, who in turn must have at least one follower. In other words, at least one leader agent is globally reachable.

Lemma 2 ([33]). According to Assumption 1, each member of $-L_1^{-1}L_2$ is non-negative, and positive real components can be found in each L_1 's eigenvalue. In addition, the matrix $-L_1^{-1}L_2$ has row sums of 1.

Definition 2 ([32]). Let the actual vector space \mathbb{R}^n be represented by $X = \{x_1, x_2, \dots, x_n\}$. The convexity of the hull of X is represented by $C_O(X)$, and defined as:

$$C_O(X) = \left\{ \sum_{i=1}^n \lambda_i x_i \mid x_i \in X, \lambda_i > 0, \sum_{i=1}^n \lambda_i = 1 \right\} \tag{6}$$

Definition 3. Multi-agent systems (3) and (4) achieve bilateral leader–follower consensus if agent i ($i = 1, \dots, M$) satisfies the following conditions:

$$\left\{ \begin{array}{l} \lim_{t \rightarrow t_f} \left\| \sum_{j=1}^N a_{ij}(x_i(t) - x_j(t)) \right\| \leq c, \\ \left\| \sum_{j=1}^N a_{ij}(x_i(t) - x_j(t)) \right\| \leq c, \quad t > t_f \\ \lim_{t \rightarrow \infty} \left\| \sum_{j=1}^N a_{ij}(x_i(t) - x_j(t)) \right\| = 0. \end{array} \right. \tag{7}$$

where c is a known constant.

The control protocol is designed using a completely distributed event-triggered technique to reduce the amount of system resources used. According to the definition:

$$\bar{x}_i(t) = \sum_{j=1}^N a_{ij}(x_i(t) - x_j(t)), \quad i \in F \tag{8}$$

$$e_i(t) = \bar{x}_i(t_k^i) - \bar{x}_i(t) \tag{9}$$

where the event-triggered condition determines the k th sample instant for follower i . The following describes the event-triggering conditions for follower i

$$f_i = \|Ke_i(t)\|^2 - \frac{\theta}{\varphi(t) + 1} \|K\bar{x}_i(t)\|^2 \tag{10}$$

θ is a constructive constant, and a time-varying function is $\varphi(t)$. Equation (10) determines the sample period,

$$t_{k+1}^i = \inf_{t > t_k^i} \{t \mid f_i(e_i(t), \bar{x}_i(t), t) = 0\} \tag{11}$$

where $i = 1, \dots, M, k \in \mathbb{N}$, and $t_0^i = 0$.

In order to achieve containment control, fixed time, and reduce communication burden, the controller is designed by using a time reference generator and event trigger. The event-triggered containment control framework for multi-agent systems based on wireless sensor networks and time base generators is shown in Figure 1. The follower obtains local information through the communication network, calculates the relative state error, and analyzes whether it satisfies the trigger condition, according to the trigger function, and then updates the control input. The control input's UI can be transmitted from the controller i to the actuator i , and then the follower state is controlled and uploaded to the communication network.

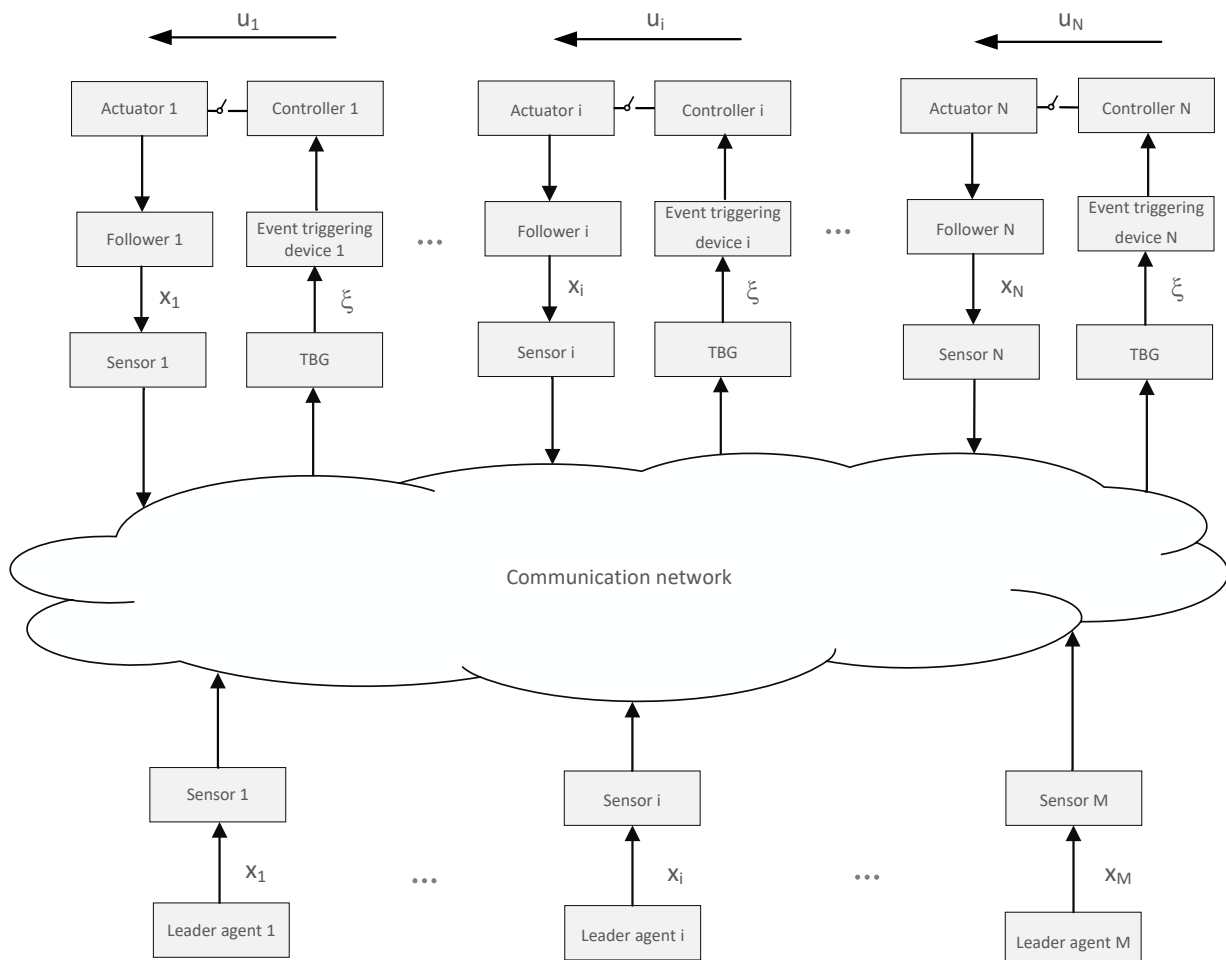


Figure 1. Event-triggered containment control algorithm for multi-agent systems based on wireless sensor networks and time base generators.

3. Main Results

This section suggests an event-triggered containment control procedure based on relative information perception for the realistic consensus with a predetermined leader. The follower (ii) control protocol is created as

$$u_i(t) = -(\varphi(t) + 1)K\bar{x}_i(t_k^i) \tag{12}$$

where K is an adequate dimensional constant matrix.

So,

$$u(t) = -(\varphi(t) + 1)(I_M \otimes K)(e(t) + \bar{x}(t)) \tag{13}$$

where $u(t) = \text{col}\{u_1(t), \dots, u_M(t)\}$, $e(t) = \text{col}\{e_1(t), \dots, e_M(t)\}$, and $\bar{x}(t) = \text{col}\{\bar{x}_1(t), \dots, \bar{x}_M(t)\}$. The control protocol can address the system containment control issue, given the following conditions.

Theorem 1. *If there is a control protocol u_i , such that all follower states asymptotically converge to the convex hull created by the leader states, then system (3) solves the containment control issue for any beginning conditions $x_i(0)$, $i \in F$, i.e.,*

$$\lim_{t \rightarrow \infty} (x_f(t) - \omega(t)) = 0 \tag{14}$$

where $\omega(t) = (-L_1^{-1}L_2 \otimes e^{At}) \begin{bmatrix} x_{M+1}(0) \\ \vdots \\ x_N(0) \end{bmatrix}$.

By substituting Equation (4) into Equation (3), we obtain:

$$\begin{cases} \dot{x}_i(t) = Ax_i(t) + Bu_i(t), & i \in F \\ \dot{x}_i(t) = Ax_i(t), & i \in E \end{cases} \tag{15}$$

where $x_f = [x_1^T \dots x_M^T]^T$, $x_l = [x_{M+1}^T \dots x_N^T]^T$.

By substituting Equation (13) into Equation (15), it can be stated succinctly as follows:

$$\begin{cases} \dot{x}_f = (I_M \otimes A)x_f - (\varphi(t) + 1)(I_M \otimes BK)(e(t) + \bar{x}(t)), \\ \dot{x}_l = (I_M \otimes A)x_l, \end{cases} \tag{16}$$

where $l \in E, f \in F$.

In accordance with the meaning of $\bar{x}_i(t)$, we have

$$\bar{x} = (L_1 \otimes I_M)\dot{x}_f + (L_2 \otimes I_M)\dot{x}_l \tag{17}$$

where $\bar{x} = [\bar{x}_1^T, \dots, \bar{x}_M^T]^T$.

Taking the derivative of Equation (16), we have

$$\begin{aligned} \dot{\bar{x}} &= (L_1 \otimes I_M)\dot{x}_f + (L_2 \otimes I_M)\dot{x}_l \\ &= (I_M \otimes A)\bar{x} - (\varphi(t) + 1)(L_1 \otimes BK)(e + \bar{x}) \end{aligned} \tag{18}$$

where $e = [e_1^T, \dots, e_M^T]^T$

Theorem 2. *To achieve an actual fixed-time leader following consensus under Assumptions 1 and 2, the requirements that follow have to be satisfied:*

1. Let us find a positive definite matrix $P \in \mathbb{R}^{n_x \times n_x}$ that satisfies:

$$A^T P + PA - \lambda_{\min}(L_1)(1 - \theta)PBB^T P \leq -Q \tag{19}$$

2. $K = B^T P$.
3. $\varphi(t) = \frac{\lambda_{\max}(P)\xi(t)}{\lambda_{\min}(L_1)(1-\xi(t)+\delta)q}$, $q = \frac{\lambda_{\min}(Q)}{\lambda_{\min}(L_1)(1-\theta)}$.

where the constant $0 < \theta < 1$ and $Q > 0$ is a matrix with a positive definite, respectively.

Proof of Theorems 1 and 2. The candidate function for the Lyapunov described below is

$$V(t) = \frac{1}{2} \bar{x}^T(t) P \bar{x}(t) \tag{20}$$

The $V(t)$ derivative in Equation (18), which occurs when $0 \leq t \leq t_f$, is given as

$$\begin{aligned} \dot{V}(t) &= \bar{x}^T(t) (I_M \otimes P) \dot{\bar{x}}(t) \\ &= \frac{1}{2} \bar{x}^T(t) (I_M \otimes (A^T P + PA)) \bar{x}(t) \\ &\quad - (\varphi(t) + 1) \bar{x}^T(t) (L_1 \otimes PBB^T P) e(t) \\ &\quad - (\varphi(t) + 1) \bar{x}^T(t) (L_1 \otimes PBB^T P) \bar{x}(t) \end{aligned} \tag{21}$$

In addition,

$$\begin{aligned} & - (\varphi(t) + 1) \bar{x}^T(t) (L_1 \otimes PBB^T P) e(t) \\ & \leq \frac{1}{2} (\varphi(t) + 1) \bar{x}^T(t) (L_1 \otimes PBB^T P) \bar{x}(t) \\ & \quad + \frac{1}{2} (\varphi(t) + 1) e^T(t) (L_1 \otimes PBB^T P) e(t) \end{aligned} \tag{22}$$

By substituting Equation (22) into Equation (21), we obtain

$$\begin{aligned} \dot{V}(t) &\leq \frac{1}{2} \bar{x}^T(t) (I_M \otimes (A^T P + PA)) \bar{x}(t) \\ &\quad + \frac{1}{2} (\varphi(t) + 1) \bar{x}^T(t) (L_1 \otimes PBB^T P) \bar{x}(t) \\ &\quad + \frac{1}{2} (\varphi(t) + 1) e^T(t) (L_1 \otimes PBB^T P) e(t) \\ &\quad - (\varphi(t) + 1) \bar{x}^T(t) (L_1 \otimes PBB^T P) \bar{x}(t) \end{aligned} \tag{23}$$

$$\begin{aligned} &\leq \frac{1}{2} \bar{x}^T(t) (I_M \otimes (A^T P + PA)) \bar{x}(t) \\ &\quad - \frac{1}{2} (\varphi(t) + 1) \bar{x}^T(t) (L_1 \otimes PBB^T P) \bar{x}(t) \\ &\quad + \frac{1}{2} (\varphi(t) + 1) e^T(t) (L_1 \otimes PBB^T P) e(t) \\ &\quad + \gamma(t) \bar{x}^T(t) (L_1 \otimes (A^T P + PA)) \bar{x}(t) \end{aligned} \tag{24}$$

where $\gamma(t) = \frac{\varphi(t)}{2(1-\theta)}$.

In accordance with event-triggered condition (6), we have

$$\|Ke_i(t)\|^2 \leq \frac{\theta}{\varphi(t) + 1} \|K\bar{x}_i(t)\|^2 \tag{25}$$

Therefore,

$$\|(L_1 \otimes K)e(t)\|^2 \leq \frac{\theta}{\varphi(t) + 1} \|(L_1 \otimes K)\bar{x}_i(t)\|^2. \tag{26}$$

By substituting Equation (26) into Equation (25), we discover:

$$\begin{aligned} \dot{V}(t) &\leq \frac{1}{2} \bar{x}^T(t) (I_M \otimes (A^T P + PA)) \bar{x}(t) \\ &\quad - \frac{1}{2} (\varphi(t) + 1) \bar{x}^T(t) (L_1 \otimes PBB^T P) \bar{x}(t) \\ &\quad + \frac{\theta}{2} \bar{x}^T(t) (L_1 \otimes PBB^T P) \bar{x}(t) \\ &\quad + \gamma(t) \bar{x}^T(t) (L_1 \otimes (A^T P + PA)) \bar{x}(t) \\ &\leq \frac{1}{2} \bar{x}^T(t) (I_M \otimes (A^T P + PA \\ &\quad - \lambda_{\min}(L1)(1 - \theta)PBB^T P)) \bar{x}(t) \\ &\quad + \gamma(t) \bar{x}^T(t) (L_1 \otimes (A^T P + PA \\ &\quad - \lambda_{\min}(L1)(1 - \theta)PBB^T P)) \bar{x}(t) \end{aligned} \tag{27}$$

According to (19), there are

$$\begin{aligned} \dot{V}(t) &\leq -\gamma(t) \bar{x}^T(t) (L_1 \otimes Q) \bar{x}(t) \\ &\leq -\frac{\varphi(t) \lambda_{\min}(L1) q}{\lambda_{\max}(P)} \\ &= -k_1(t) V(t) \end{aligned} \tag{28}$$

where $k_1(t) = \frac{\dot{\xi}(t)}{1 - \xi(t) + \delta}$. Lemma 1 states that we can directly obtain $V(t) \leq \frac{\delta}{1 + \delta} V(0)$. Therefore,

$$\lim_{t \rightarrow t_f} \left\| \sum_{j=1}^N a_{ij} (x_i(t) - x_j(t)) \right\| \leq \sqrt{\frac{2\delta V(0)}{\lambda_{\min}(P) \lambda_{\min}(L1)}} \tag{29}$$

When $t \geq t_f$, we can obtain the following equation:

$$\dot{\bar{x}} = (I_M \otimes A) \bar{x} - (L_1 \otimes BK)(e(t) + \bar{x}(t)) \tag{30}$$

Using Equation (30) and the time-derivative of $V(t)$, we obtain

$$\begin{aligned} \dot{V}(t) &= \frac{1}{2} \bar{x}^T(t) (I_M \otimes (A^T P + PA)) \bar{x}(t) \\ &\quad - \bar{x}^T(t) (L_1 \otimes PBB^T P) e(t) \\ &\quad - \bar{x}^T(t) (L_1 \otimes PBB^T P) \bar{x}(t) \\ &\leq \frac{1}{2} \bar{x}^T(t) (I_M \otimes (A^T P + PA)) \bar{x}(t) \\ &\quad - \frac{1}{2} \bar{x}^T(t) (L_1 \otimes PBB^T P) \bar{x}(t) \\ &\quad - \frac{1}{2} e^T(t) (L_1 \otimes PBB^T P) e(t) \\ &\leq \frac{1}{2} \bar{x}^T(t) \left(I_M \otimes \left(A^T P + PA \right. \right. \\ &\quad \left. \left. - \lambda_{\min}(L1)(1 - \theta)PBB^T P \right) \right) \bar{x}(t) \\ &\leq -\frac{1}{2} \bar{x}^T(t) (L_1 \otimes Q) \bar{x}(t) \\ &\leq -k_2 V(t) \end{aligned} \tag{31}$$

The equation for k_2 is given by

$$k_2 = \frac{\lambda_{\min}(Q)\lambda_{\min}(L1)}{\lambda_{\max}(P)} \tag{32}$$

Consequently, it is evident that

$$V(t) \leq V(t_f)e^{-k_2(t-t_f)} \tag{33}$$

Hence, the result is:

$$\lim_{t \rightarrow t_f} \left\| \sum_{j=1}^N a_{ij}(x_i(t) - x_j(t)) \right\| = 0 \tag{34}$$

Thus, Theorem 2 is proved.

The eigenvalues of L_1 are known to all have positive real portions under the assumption of Condition 3 and according to Lemma 2. From Equation (17), it follows that

$$\lim_{t \rightarrow \infty} \left\| \sum_{j=1}^N a_{ij}(x_i(t) - x_j(t)) \right\| = 0 \tag{35}$$

This implies

$$\lim_{t \rightarrow \infty} \left\| \left(x_f(t) - (-L_1^{-1}L_2 \otimes I_{n_x})x_1(t) \right) \right\| = 0 \tag{36}$$

By substituting $x_i(t) = e^{At}x_i(0)$ for $i \in E$, we can obtain $\lim_{t \rightarrow \infty} (x_f(t) - \omega(t)) = 0$

where $\omega(t) = (-L_1^{-1}L_2 \otimes e^{At}) \begin{bmatrix} x_{M+1}(0) \\ \vdots \\ x_N(0) \end{bmatrix}$.

Thus, Theorem 1 is proved. \square

Remark 2. In this study, the term "fixed-time control" refers to the use of TBG control protocols to make sure the system's status changes to the intended level within a given time interval t_f . Consensus can be achieved through the $-K\bar{x}_i(t_k^i)$ term in the control protocol (12). A key advantage of our approach, compared to many existing fixed-time containment control studies, is the relatively small initial control input, which effectively reduces system costs.

Remark 3. The time delay may cause oscillation, instability, or slow convergence. This is a challenge for the design of control systems. It is necessary to consider the time delay influence on the stability of the system. The shortcoming of this paper is that the communication delay is not considered. We plan to further explore this topic in future work to improve the control performance and propose better solutions to deal with communication delays.

Remark 4. Event-triggered containment control can effectively reduce communication and computing loads and improve the energy efficiency of the system. The containment control based on the time reference generator can ensure that each agent in the system operates and communicates according to a unified time axis, so as to achieve coordinated and synchronous control. The choice of the appropriate method for the two control schemes depends on the specific application scenarios and system requirements, as well as the trade-off considerations for the communication load, energy efficiency, and synchronization requirements.

Theorem 3. When neither party can reach an agreement, Zeno behavior is circumvented in control protocol (12) and under the event-triggering condition (10).

Proof of Theorem 3. For the time interval $0 \leq t \leq t_f$, where

$$\frac{d\|Ke_i(t)\|^2}{dt} = -2e_i^T(t)K^TK\dot{\bar{x}}_i(t) \tag{37}$$

The prior study led to the conclusion that $e_i(t)$ has an upper bound $\vartheta = \max(|e_i(t)|)$. By using Equation (18), we can further derive

$$\dot{\bar{x}}_i(t)_{\max} = \lambda_{\max}(A)\omega - (\varphi_{\max} + 1)\psi(\vartheta + \omega) \tag{38}$$

The following expression can be used to obtain the greatest value of ω , of $\bar{x}_i(t)$, in Equation (29):

$$\omega = \sqrt{\frac{2\delta V(0)}{\lambda_{\min}(P)\lambda_{\min}(L1)}} \tag{39}$$

Furthermore, ψ represents the maximum value of $L1 \otimes BK$, and φ_{\max} represents the maximum value of $\varphi(t)$, which can be determined using Theorem 2.

Therefore, we can conclude that

$$\frac{d\|Ke_i(t)\|^2}{dt} \leq -2\vartheta\|K^TK\|(\lambda_{\max}(A)\omega - (\varphi(t)_{\max} + 1)\psi(\vartheta + \omega)) \tag{40}$$

Define $\Phi_i = -2\vartheta\|K^TK\|(\lambda_{\max}(A)\omega - (\varphi(t)_{\max} + 1)\psi(\vartheta + \omega))$. Thus, we have $\frac{d\|Ke_i(t)\|^2}{dt} \leq \Phi_i \leq \infty$.

Therefore, we obtain

$$\|Ke_i(t)\|^2 \leq \Phi_i(t - t_{k_i}^i) \tag{41}$$

where $t_{k_i}^i < t$ represents the most recent event-triggered moment of follower i at time t .

Thus, $k_i^i = \arg \min_{l \in N; t \geq t_l^i} \{t - t_l^i\}$.

Furthermore, we can deduce that

$$\|Ke_i(t_{k_{i+1}^i}^i)\|^2 \leq \Phi_i(t_{k_{i+1}^i}^i - t_{k_i}^i) \tag{42}$$

where $t_{k_{i+1}^i}^i$ represents the next event-triggered instant.

By Equation (10), we can deduce that

$$\begin{aligned} \|Ke_i(t_{k_{i+1}^i}^i)\|^2 &= \frac{\theta}{\varphi(t_{k_{i+1}^i}^i) + 1} \|K\bar{x}_i(t_{k_{i+1}^i}^i)\|^2 \\ &\geq \frac{\theta}{\varphi_{\max} + 1} \|K\bar{x}_i(t_{k_{i+1}^i}^i)\|^2 \\ &> 0 \end{aligned} \tag{43}$$

Therefore, we can conclude that $t_{k_{i+1}^i}^i - t_{k_i}^i \geq \Phi_i^{-1} \|Ke_i(t_{k_{i+1}^i}^i)\| > 0$.

When $t > t_f$, similar to the example $0 \leq t \leq t_f$, the study of inter-event timings and the conclusion $t_{k_{i+1}^i}^i - t_{k_i}^i > 0$ can be directly obtained. Hence, Zeno behavior can be avoided.

Theorem 3 has been fully demonstrated. \square

4. Simulation Example

To check the accuracy of the theoretical findings, we employ a simulation example in this section. Consider a multi-agent system with eight followers and four leaders to demonstrate the use of the control protocol. The dynamics of each agent are described by Equations (3) and (4), where $x_f(t), x_l(t) \in \mathbb{R}^2, f = 1, \dots, 8, l = 1, 2, 3, 4$. The initial states of each follower and leader are set to $x_{f_j}(0) \in (-2; 2), x_{l_1}(0) = (3; -2), x_{l_2}(0) = (-4; 4)$,

$x_{l3}(0) = (1; -1), x_{l4}(0) = (2; -2)$. It is possible to choose the parameter θ , system matrices A and B , and matrix Q with positive definiteness, as follows:

$$\theta = 0.5.$$

$$A = \begin{bmatrix} -1 & 0 \\ 1 & 0 \end{bmatrix}, B = \begin{bmatrix} 0.1 \\ 1 \end{bmatrix}, Q = \begin{bmatrix} 0.3 & 0 \\ 0 & 0.3 \end{bmatrix}.$$

According to inequality (19), the conclusion can be obtained as

$$P = \begin{bmatrix} 4.4448 & 4.1448 \\ 4.1448 & 4.1448 \end{bmatrix}.$$

Figure 2 depicts the topology of the communication. While the other nodes represent the followers, nodes 1, 2, and 3 represent the leaders.

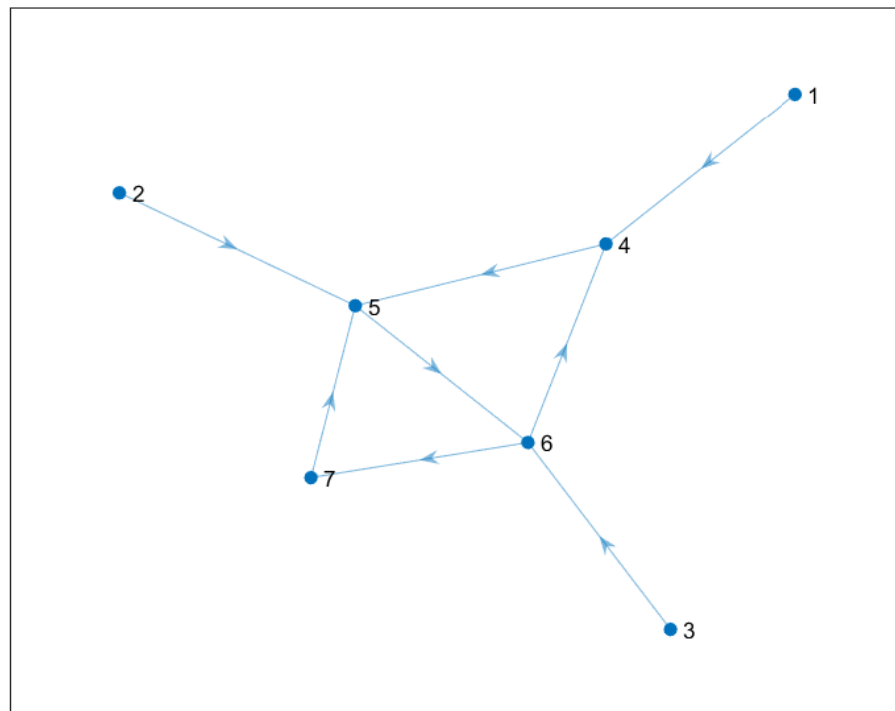


Figure 2. Communication topology.

Clearly, Assumption 1 is satisfied. Corresponding to Equation (3),

$$L1 = \begin{bmatrix} 2 & 0 & 0 & -1 & 0 & 0 & -1 & 0 \\ -1 & 3 & 0 & 0 & 0 & 0 & -1 & -1 \\ 0 & 0 & 1 & 0 & 0 & 0 & -1 & 0 \\ 0 & -1 & 0 & 2 & 0 & 0 & 0 & 0 \\ 0 & 0 & -1 & 0 & 2 & 0 & 0 & 0 \\ 0 & 0 & 0 & 0 & -1 & 2 & -1 & 0 \\ 0 & 0 & 0 & 0 & 0 & -1 & 2 & 0 \\ 0 & -1 & 0 & -1 & 0 & 0 & -1 & 4 \end{bmatrix}$$

$$L2 = \begin{bmatrix} 0 & 0 & 0 & 0 \\ 0 & 0 & 0 & 0 \\ 0 & 0 & 0 & 0 \\ -1 & 0 & 0 & 0 \\ 0 & 0 & -1 & 0 \\ 0 & 0 & 0 & 0 \\ 0 & -1 & 0 & 0 \\ 0 & 0 & 0 & -1 \end{bmatrix}$$

According to Definition 2, TBG $\zeta(t)$ can be chosen as

$$\zeta(t) = \begin{cases} \frac{10}{4^6}t^6 - \frac{24}{4^5}t^5 + \frac{24}{4^3}t^4, & 0 \leq t \leq t_f \\ 1, & t > t_f \end{cases}$$

$t_f = 4$ s in this case.

Figure 3 shows the change in the state trajectory of the multi-agent system. It can be seen that all followers gradually converge to the convex hull formed by the leader state, indicating that the control method is effective. The control input is shown in Figure 4. When $t = 4$ s, the control input tends to be stable, indicating that the controller remains stable in the subsequent period, which further proves that the containment control problem of the system is solvable (3). Figure 5 shows the instants and intervals of event triggering. The line indicates whether the event is triggered (if triggered, there are line circles), and the vertical distance of a single circle is the interval time between the triggering and the previous moment. It can be seen that the followers have no Zeno phenomenon (i.e., continuous points) and the trigger interval is long, indicating that the control scheme effectively reduces the communication.

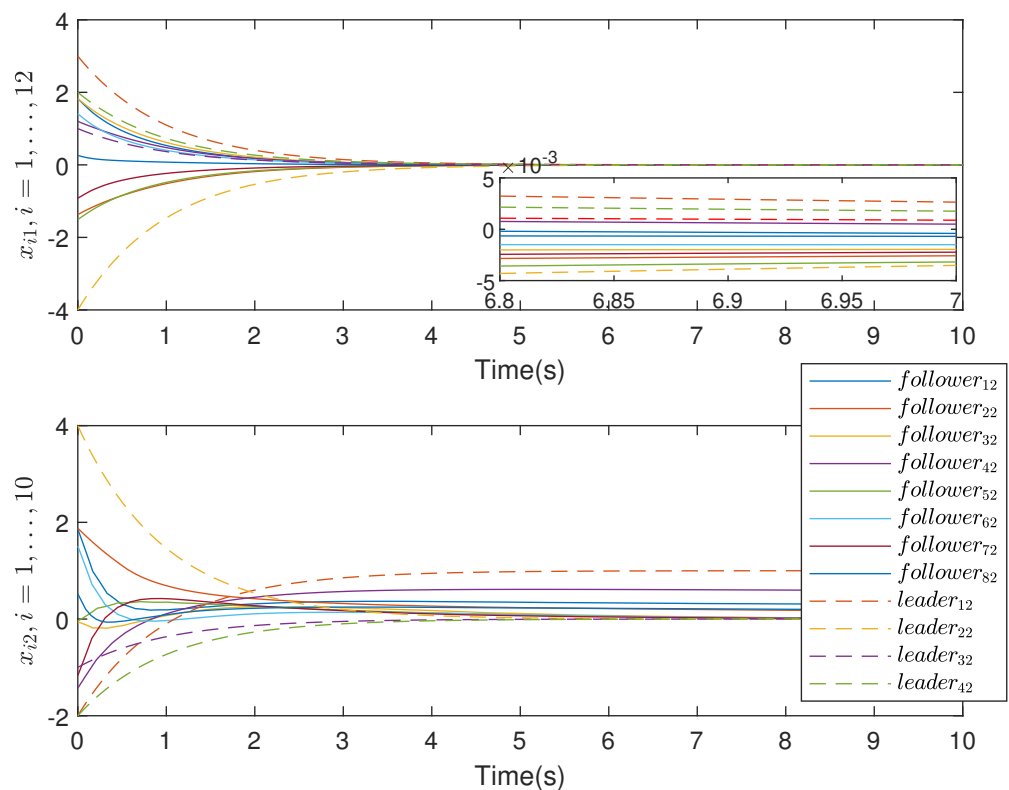


Figure 3. State trajectory under the control protocol.

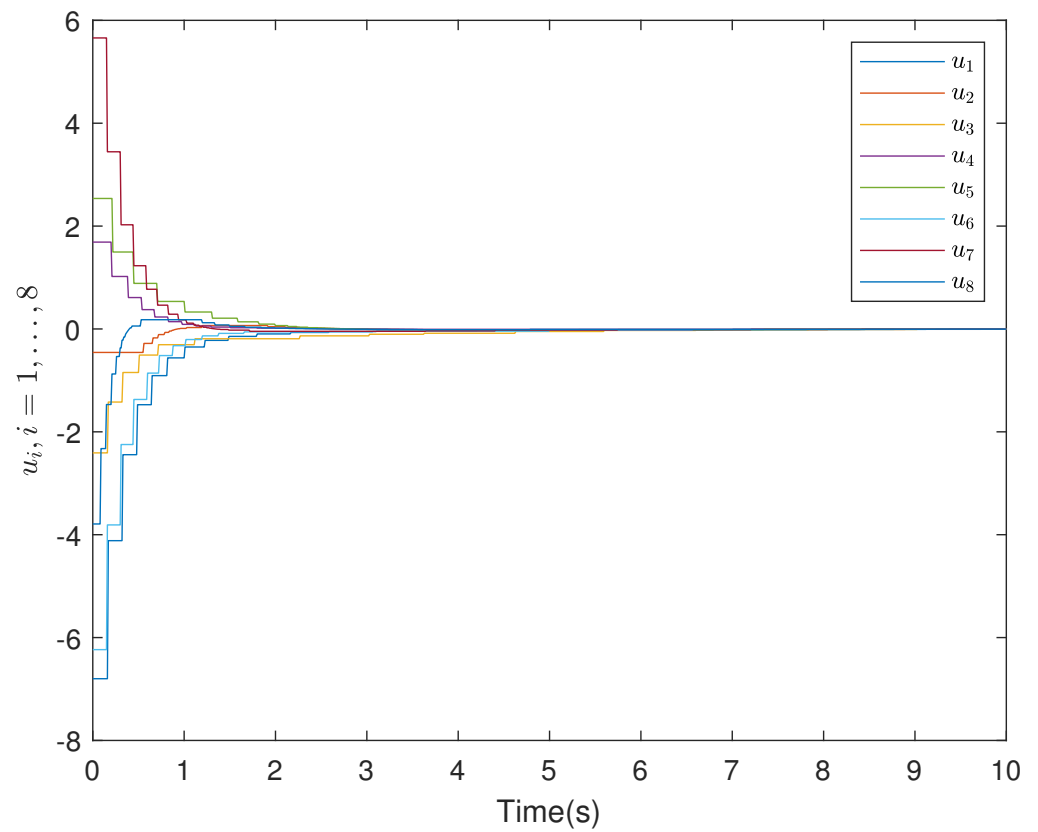


Figure 4. Evolution of the control input under the control protocol.

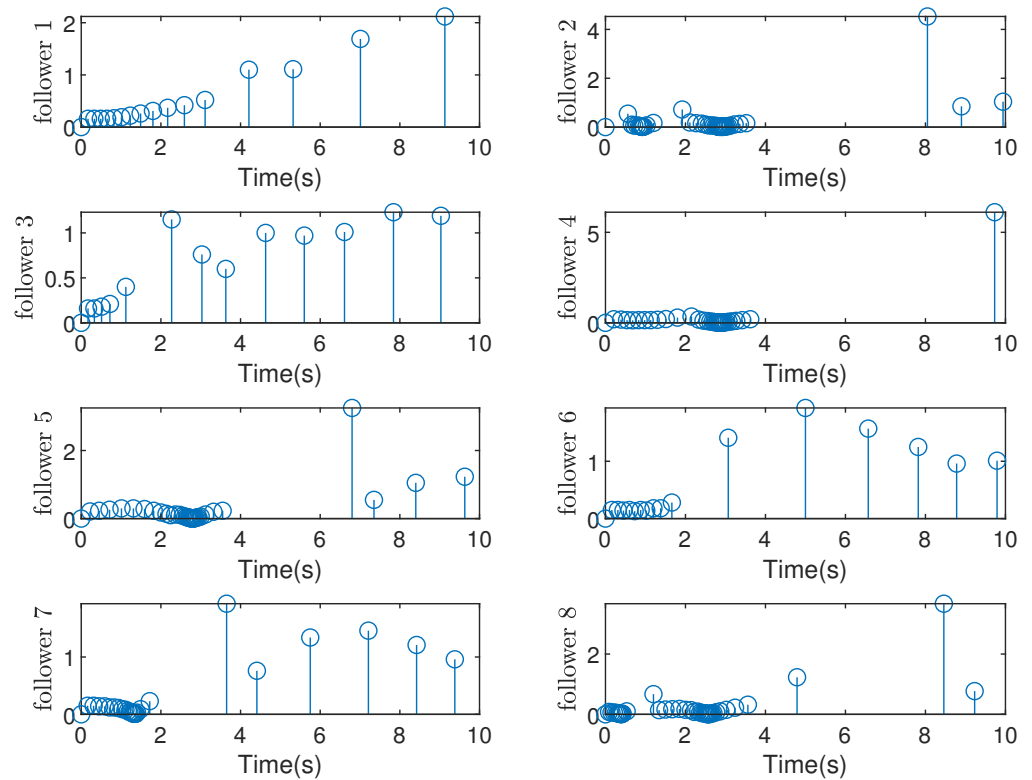


Figure 5. Moments and intervals triggered by events.

5. Conclusions

This research suggests an event-triggered containment control algorithm that is fully distributed based on wireless sensor networks and a time base generator (TBG) to effectively address the timing-consistent containment control issue in directed, fixed-topology multi-agent systems. The control protocol aims to ensure consensus consistency in the system by reducing the state divergence to a specific level within a known stable time. Through analysis and proof using Lyapunov methods and matrix inequalities, it is demonstrated that all follower agent states can converge within the hull of the leader state when the suggested control technique is used, which is convex. In comparison with traditional methods, the algorithm presented in this study enables faster convergence of multi-agent system followers to the convex hull of the leader while avoiding Zeno behavior. Finally, simulated examples are used to show that the suggested control strategy is preferable. The shortcoming is that the time delay problem is not considered in this paper. In future research, it will be necessary to consider the time delay influence on multi-agent systems.

Author Contributions: Conceptualization, L.W.; methodology, G.C.; software, R.Y.; validation, T.L.; data curation, L.W.; writing—original draft preparation, L.W.; writing—review and editing, R.Y. All authors have read and agreed to the published version of the manuscript.

Funding: This work was supported by the Natural Science Foundation of the Higher Education Institutions of Jiangsu Province (no. 22KJB120009), the Start-up Fund for Introducing Talent of Wuxi University (no. 2023r027, no. 2022r025, no. 2021r045), the Wuxi Innovation and Entrepreneurship Fund ‘Taihu Light’ Science and Technology (Fundamental Research) Project (grant no. K20221045), and the Innovative Leading Talents in the Universities of Xishan Talents Program (no. 2022xsyc001).

Informed Consent Statement: Not applicable.

Data Availability Statement: All data generated or analyzed during this study are included in this article.

Conflicts of Interest: The authors declare no conflict of interest.

References

- Xu, B.; Lu, M.; Zhang, H.; Pan, C. A Novel Multi-Agent Model for Robustness with Component Failure and Malware Propagation in Wireless Sensor Networks. *Sensors* **2021**, *21*, 4873. [[CrossRef](#)] [[PubMed](#)]
- Peng, Z.; Liu, L.; Wang, J. Output-Feedback Flocking Control of Multiple Autonomous Surface Vehicles Based on Data-Driven Adaptive Extended State Observers. *IEEE Trans. Cybern.* **2021**, *51*, 4611–4622. [[CrossRef](#)] [[PubMed](#)]
- Ibuki, T.; Wilson, S.; Yamauchi, J.; Fujita, M.; Egerstedt, M. Optimization-Based Distributed Flocking Control for Multiple Rigid Bodies. *IEEE Robot. Autom. Lett.* **2020**, *5*, 1891–1898. [[CrossRef](#)]
- Abichandani, P.; Speck, C.; Bucci, D.; McIntyre, W.; Lobo, D. Implementation of Decentralized Reinforcement Learning-Based Multi-Quadrotor Flocking. *IEEE Access* **2021**, *9*, 132491–132507. [[CrossRef](#)]
- Stamouli, C.J.; Bechlioulis, C.P.; Kyriakopoulos, K.J. Multi-Agent Formation Control Based on Distributed Estimation With Prescribed Performance. *IEEE Robot. Autom. Lett.* **2020**, *5*, 2929–2934. [[CrossRef](#)]
- Du, X.; Li, W.; Xiao, J.; Chen, Z. Time-Varying Group Formation With Adaptive Control for Second-Order Multi-Agent Systems. *IEEE Access* **2022**, *10*, 45337–45346. [[CrossRef](#)]
- Cui, Y.; Liu, X.; Deng, X.; Wang, Q. Observer-based adaptive fuzzy formation control of nonlinear multi-agent systems with nonstrict-feedback form. *Int. J. Fuzzy Syst.* **2021**, *23*, 680–691. [[CrossRef](#)]
- Li, T.; Li, Z.; Fei, S.; Ding, Z. Second-order event-triggered adaptive containment control for a class of multi-agent systems. *ISA Trans.* **2020**, *96*, 132–142. [[CrossRef](#)]
- Zhang, J.; Yan, F.; Feng, T.; Deng, T.; Zhao, Y. Fastest containment control of discrete-time multi-agent systems using static linear feedback protocol. *Inf. Sci.* **2022**, *614*, 362–373. [[CrossRef](#)]
- Wang, D.; Wang, W. Necessary and sufficient conditions for containment control of multi-agent systems with time delay. *Automatica* **2019**, *103*, 418–423. [[CrossRef](#)]
- Li, Y.; Qu, F.; Tong, S. Observer-Based Fuzzy Adaptive Finite-Time Containment Control of Nonlinear Multiagent Systems With Input Delay. *IEEE Trans. Cybern.* **2021**, *51*, 126–137. [[CrossRef](#)] [[PubMed](#)]
- Wang, W.; Liang, H.; Pan, Y.; Li, T. Prescribed Performance Adaptive Fuzzy Containment Control for Nonlinear Multiagent Systems Using Disturbance Observer. *IEEE Trans. Cybern.* **2020**, *50*, 3879–3891. [[CrossRef](#)] [[PubMed](#)]
- Lu, Y.; Dong, X.; Li, Q.; Lu, J.; Ren, Z. Time-Varying Group Formation-Containment Tracking Control for General Linear Multiagent Systems With Unknown Inputs. *IEEE Trans. Cybern.* **2022**, *52*, 11055–11067. [[CrossRef](#)] [[PubMed](#)]

14. Liu, Y.; Zhang, H.; Sun, J.; Wang, Y. Adaptive Fuzzy Containment Control for Multi agent Systems With State Constraints Using Unified Transformation Functions. *IEEE Trans. Fuzzy Syst.* **2022**, *30*, 162–174. [[CrossRef](#)]
15. Chen, Z.; Cai, L.; Zhao, C. Convergence time of average consensus with heterogeneous random link failures. *Automatica* **2021**, *127*, 109496. [[CrossRef](#)]
16. Ullah, S.; Khan, L.; Sami, I.; Ullah, N. Consensus-Based Delay-Tolerant Distributed Secondary Control Strategy for Droop Controlled AC Microgrids. *IEEE Access* **2021**, *9*, 6033–6049. [[CrossRef](#)]
17. Hu, A.H.; Wang, Y.; Cao, J.D.;Alsaedi, A. Event-triggered bipartite consensus of multi-agent systems with switching partial couplings and topologies. *Inf. Sci.* **2020**, *521*, 1–13. [[CrossRef](#)]
18. Sun, K.; Qiu, J.; Karimi, H.R.;Fu, Y. Event-triggered robust fuzzy adaptive finite-time control of nonlinear systems with prescribed performance. *IEEE Trans. Fuzzy Syst.* **2020**, *29*, 1460–1471. [[CrossRef](#)]
19. Girard, A. Dynamic triggering mechanisms for event-triggered control. *IEEE Trans. Autom. Control* **2015**, *60*, 1992–1997. [[CrossRef](#)]
20. Zhao, D.; Wang, Z.D.; Wei, G.L.;Han, Q.L. A dynamic event-triggered approach to observer-based PID security control subject to deception attacks. *Automatica* **2020**, *120*, 109128. [[CrossRef](#)]
21. Cheng, W.; Zhang, K.; Jiang, B.; Ding, S.X. Fixed-Time Fault Tolerant Formation Control for Heterogeneous Multi-Agent Systems With Parameter Uncertainties and Disturbances. *IEEE Trans. Circuits Syst. I Regul. Pap.* **2021**, *68*, 2121–2133. [[CrossRef](#)]
22. Sun, Y.; Shi, P.; Lim, C.C. Event-triggered sliding mode scaled consensus control for multi-agent systems. *J. Frankl. Inst.* **2022**, *359*, 981–998. [[CrossRef](#)]
23. Ma, T.; Zhang, Z.; Cui, B. Impulsive consensus of nonlinear fuzzy multi-agent systems under DoS attack. *Nonlinear Anal. Hybrid Syst.* **2022**, *44*, 101155. [[CrossRef](#)]
24. Liang, H.; Guo, X.; Pan, Y.; Huang, T. Event-Triggered Fuzzy Bipartite Tracking Control for Network Systems Based on Distributed Reduced-Order Observers. *IEEE Trans. Fuzzy Syst.* **2021**, *29*, 1601–1614. [[CrossRef](#)]
25. Li, X.; Tang, Y.; Karimi, H.R. Consensus of multi-agent systems via fully distributed event-triggered control. *Automatica* **2020**, *116*, 108898. [[CrossRef](#)]
26. Selvaraj, P.; Kwon, O.M.; Lee, S.H.;Sakthivel, R. Equivalent-input-disturbance estimator-based event-triggered control design for master–slave neural networks. *Neural Netw.* **2021**, *143*, 413–424. [[CrossRef](#)]
27. Song, G.; Shi, P.; Agarwal, R.K. Fixed-time sliding mode cooperative control for multiagent networks via event-triggered strategy. *Int. J. Robust Nonlinear Control* **2021**, *31*, 21–36. [[CrossRef](#)]
28. Ni, J. Fixed-time terminal sliding mode tracking protocol design for high-order multiagent systems with directed communication topology. *ISA Trans.* **2022**, *124*, 444–457. [[CrossRef](#)]
29. Zhao, M.; Gu, C.; Zhao, L.; Liu, Y. Fixed-time leader-following consensus tracking control for nonlinear multi-agent systems under jointly connected graph. *Entropy* **2022**, *24*, 1130. [[CrossRef](#)]
30. Li, G.F.; Wu, Y.J.; Liu, X.C. Adaptive fixed-time consensus tracking control method for second-order multi-agent systems with disturbances. *J. Frankl. Inst.* **2020**, *357*, 1516–1531. [[CrossRef](#)]
31. Hao, L.; Zhan, X.; Wu, J.; Han, T.; Yan, H. Fixed-time group consensus of nonlinear multi-agent systems via pinning control. *Int. J. Control Autom. Syst.* **2021**, *19*, 200–208. [[CrossRef](#)]
32. Zou, W.; Qian, K.; Xiang, Z. Fixed-Time Consensus for a Class of Heterogeneous Nonlinear Multiagent Systems. *Trans. Circuits Syst.* **2020**, *67*, 1279–1283. [[CrossRef](#)]
33. Du, H.; Wen, G.; Cheng, Y.; Lu, J. Distributed fixed-time consensus for nonlinear heterogeneous multi-agent systems. *Automatica* **2020**, *113*, 108797. [[CrossRef](#)]
34. Ning, B.; Han, Q.L.; Zuo, Z. Practical fixed-time consensus for integrator-type multi-agent systems: A time base generator approach. *Automatica* **2019**, *105*, 406–414. [[CrossRef](#)]
35. Meng, Z.Y.; Ren, W.; You, Z. Distributed finite-time attitude containment control for multiple rigid bodies. *Automatica* **2010**, *46*, 2092–2099. [[CrossRef](#)]
36. Qin, H.D.; Chen, H.; Sun, Y.C.; Wu, Z.Y. The distributed adaptive finite-time chattering reduction containment control for multiple ocean bottom flying nodes. *Int. J. Fuzzy Syst.* **2019**, *21*, 607–619. [[CrossRef](#)]

Disclaimer/Publisher’s Note: The statements, opinions and data contained in all publications are solely those of the individual author(s) and contributor(s) and not of MDPI and/or the editor(s). MDPI and/or the editor(s) disclaim responsibility for any injury to people or property resulting from any ideas, methods, instructions or products referred to in the content.